Journal of Instrumentation

PAPER • **OPEN ACCESS**

The upgrade of the ASACUSA scintillating bar detector for antiproton annihilation measurements

To cite this article: Giovanni Costantini *et al* 2023 *JINST* **18** P04013

Jinst

Published by IOP Publishing for Sissa Medialab

Received: *February 10, 2023*
Accepted: *March 17, 2023*
Published: *April 11, 2023*

The upgrade of the ASACUSA scintillating bar detector for antiproton annihilation measurements

Giovanni Costantini,[a,b] **Luca Giorleo,**[c] **Giulia Gosta,**[a,b] **Marco Leali,**[a,b] **Valerio Mascagna,**[a,b,*] **Stefano Migliorati,**[a,b] **Michela Prest,**[d,e] **Federico Ronchetti,**[d,e,1] **Luigi Solazzi,**[c,b] **Erik Vallazza**[e] **and Luca Venturelli**[a,b]

[a] *Dipartimento di Ingegneria dell'Informazione, Università degli Studi di Brescia, Via Branze 38, 25123 — Brescia, Italy*
[b] *INFN — Sezione di Pavia, Via Bassi 6, 27100 — Pavia, Italy*
[c] *Dipartimento di Ingegneria Meccanica e Industriale, Università degli Studi di Brescia, Via Branze 38, 25123 — Brescia, Italy*
[d] *Dipartimento di Scienza e Alta Tecnologia, Università degli Studi dell'Insubria, Via Valleggio 11, 22100 — Como, Italy*
[e] *INFN — Sezione di Milano Bicocca, Piazza della Scienza 3, 20126 — Milano, Italy*

E-mail: valerio.mascagna@unibs.it

Abstract: Antiproton annihilations on matter nuclei are usually detected by tracking the charged pions emitted in the process. A detector made of plastic scintillating bars have been built and used in the ASACUSA experiment for the last 10 years. Ageing, movements and transports caused stress on the internal mechanical structure and impacted mostly on the optical readout system which was eventually upgraded: the so far used multi-anode photo-multiplier tubes (PMTs) have been replaced by silicon photomultipliers (SiPM) and the front-end electronics had to be adapted to cope with the new signal formation. This work describes the design and operations of the upgrade, as well as the validation tests with cosmic rays.

Keywords: Front-end electronics for detector readout; Photon detectors for UV, visible and IR photons (solid-state); Photon detectors for UV, visible and IR photons (solid-state) (PIN diodes, APDs, Si-PMTs, G-APDs, CCDs, EBCCDs, EMCCDs, CMOS imagers, etc); Scintillators, scintillation and light emission processes (solid, gas and liquid scintillators)

[1] Currently at: Institute of Physics, Ecole Polythecnique Fédérale de Lausanne (EPFL), Lausanne, Switzerland.
[*] Corresponding author.

https://doi.org/10.1088/1748-0221/18/04/P04013

2023 JINST 18 P04013

Contents

2023 JINST 18 P04013

1 Introduction

The ASACUSA Collaboration (Atomic Spectroscopy And Collisions Using Slow Antiprotons) has been operating at the Antiproton Decelerator facility (AD) at CERN for more than 20 years. The research program aims to test fundamental symmetries and the unbalanced matter antimatter ratio in the Universe by the formation and study of antihydrogen [1–4] as well as other hybrid atoms like antiprotonic helium [5–7]. The antiproton collisions and annihilations on different nuclei is also studied.

In the antihydrogen formation experiment, as well as the collisions and annihilations measurements, the process which can be easily detected is the annihilation of the antiprotons on nuclei which typically results in emitted pions. In the first case the antiprotons delivered by the AD are slowed down, trapped and eventually mixed with positrons: the detected pions are tracked back to the annihilation vertex allowing to localize the regions where the antiptrotons are lost (annihilation on the residual gas or the beam pipe walls). In the second case the antiprotons travel in an vacuum pipe crossing a very thin foils of material (nm scale) so that a small amount of them interact through annihilations which are counted by detecting the emitted pions.

On average 5 pions are produced, 3 of which are charged, with a mean momentum around 200 MeV/c [8]. The charged pions can be easily detected by any instrument based on plastic scintillators and a proper light readout system.

A detector made of scintillating bars [9] has been used by the collaboration in different configurations. A scheme of the experimental layout used in the antihydrogen formation experiment is shown in figure 1. In this case, counting emitted pions and reconstructing the annihilation vertices were important to demonstrate the first antihydrogen atoms formation in a cusp trap [10], and in

the following years the detector was used to monitor the annihilations during the trapping operation providing a valuable tool for optimizing the antihydrogen formation procedure [11–14].

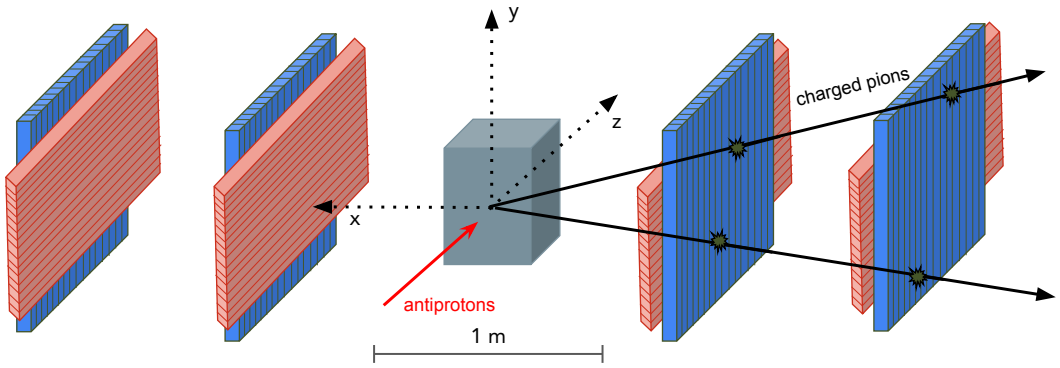

Figure 1. Sketch of the scintillating bar detector in the antihydrogen formation experiment: 8 panels are placed close to the interaction region in a XY configuration (4 couples) to allow the 3D tracking of the charged pions emerging from the antiproton annihilations on the trap walls. The trap is schematically represented by the box in the center.

Each detector sensitive panel can be deployed separately in a given position and this modular design was useful in the experiment to measure the antiproton annihilation cross sections where the geometrical acceptance had to be optimized. Measurements at different antiproton energies required different layouts around the target area and that was achievable because of the above mentioned flexibility [15–19].

2 The detector

The detector consists of panels of extruded scintillating bars made of Polystyrene Dow Styron 663 W + 1% PPO + 0.03% POPOP and white TiO2 coating [20] (a single panel is shown in figure 2). Each bar has a cross section of $1.5 \times 1.9\,\mathrm{cm}^2$ and is 96 cm long; a hole along its axis with a 2 mm groove is used to glue inside a 1 mm diameter wavelength shifting fiber (WLS) of the Y-11 type by Kuraray.[1] The fibers are then darkened, grouped into bundles of 30–32 and coupled to a 64 channel multi-anode H7546-B photomultiplier (PMT) by Hamamatsu.[2] In order to avoid cross-talk between nearby pads, only half of the PMT channels are used.

3 The frontend board and the MAROC3 ASIC

The readout of each PMT signals (after the upgrade, each SiPM ones) is performed by a front end board Board (FEB) equipped with a MAROC3 (Multi Anode ReadOut Chip 3) ASIC developed by the Omega group at LAL[3] originally for the ATLAS luminometer [21]. The chip is manufactured with the Si-Ge 0.35 µm technology, it has an effective area of $4 \times 4\,\mathrm{mm}^2$, it's enclosed in a CQFP240 package and operates with a bias voltage of 3.5 V. It is mounted on the board together with two

[1] https://www.kuraray.com/.
[2] https://www.hamamatsu.com/eu/en/index.html.
[3] https://portail.polytechnique.edu/omega.

2023 JINST 18 P04013

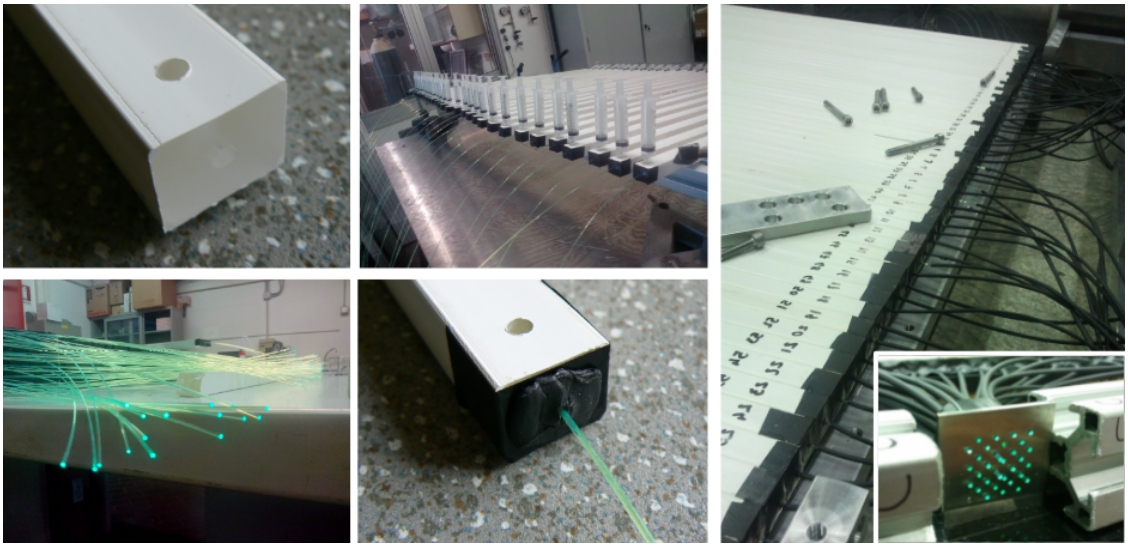

Figure 2. Illustration of how a detector single panel is composed: a scintillating bar is shown before and after gluing a WLS fiber inside (the hole used to pour in the glue through syringes is visible). The final assembly is shown on the right side of the collage, including the aluminum mask used to readout the fiber with a multi-anode PMT.

ALTERA Cyclone II FPGAs (model EP2C8Q208I8N, Altera Corporation)[4] for the configuration and the readout and a 12 bit analog-to-digital converter (ADC) circuit (model AD9220ARZ, Analog Devices).[5] The whole MAROC board is shown in figure 3. This board provides the power supply to the components and is equipped with all the needed connectors for the communication with the VME electronics (analog and digital I/O connectors and a dedicated one for the trigger signals) and a 64 pins socket for the analog input signals. The MAROC3 chip is a 64-channel input front-end circuit suited to read signals from PMTs or SiPMs and it provides a single shaped signal proportional to the input charge and 64 digital trigger outputs [22]. Each input channel has a variable gain preamplifier — with a 8-bit tunable gain, up to a factor 4 — and a low input impedance. A current mirror feeds two different signal paths, as shown in figure 4. The first one is the analog part, that consists in a RC buffer, a slow CRRC^2 tunable shaper, two sample-and-hold circuits to measure the signal amplitude and its baseline and a 5 MHz clock multiplexer. The second one is the digital part that consists in a fast shaper and a discriminator with a tunable threshold. The MAROC3 is also equipped with a Wilkinson ADC, not used in this experience. Some output pins on the FEB (visible in the upper-left part of in figure 3) allow to directly measure 8 signals made by the sum of 8 different MAROC3 channels after the preamplifier. The slow shaper feedback capacitors (300, 600 and 1200 fF) can be set via three switches independently to build the shaped signal with different widths and peak time. The gain of the input signal in the shaper can be chosen adjusting four other capacitors in the RC buffer, that should be optimized to have a good signal/noise ratio.

The above described ASIC parameters have been tested and investigated in order to ensure the feasibility of the readout of SiPMs signals instead of PMTs ones (see section 5).

[4] http://www.altera.com.
[5] http://www.analog.com.

2023 JINST 18 P04013

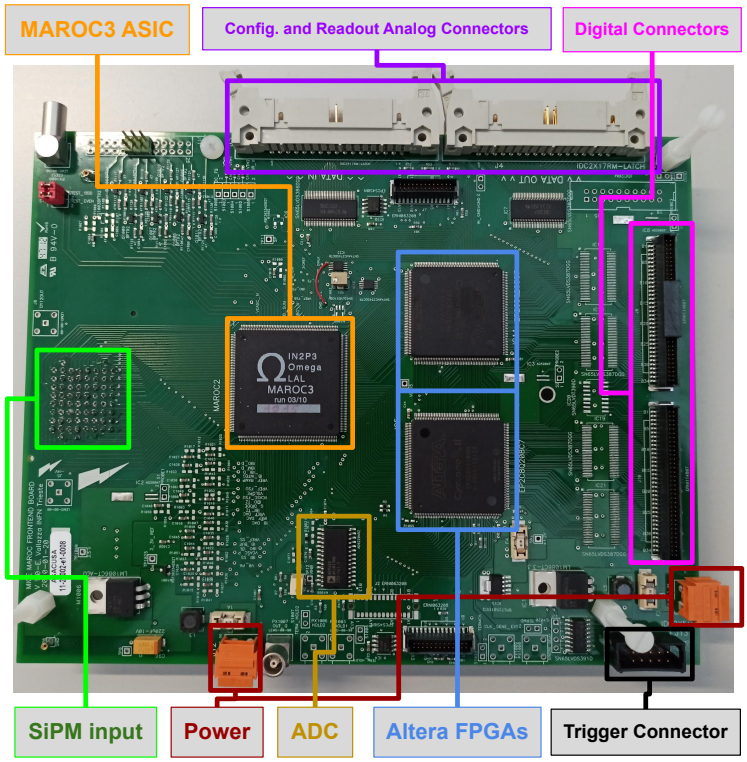

Figure 3. The MAROC front end board.

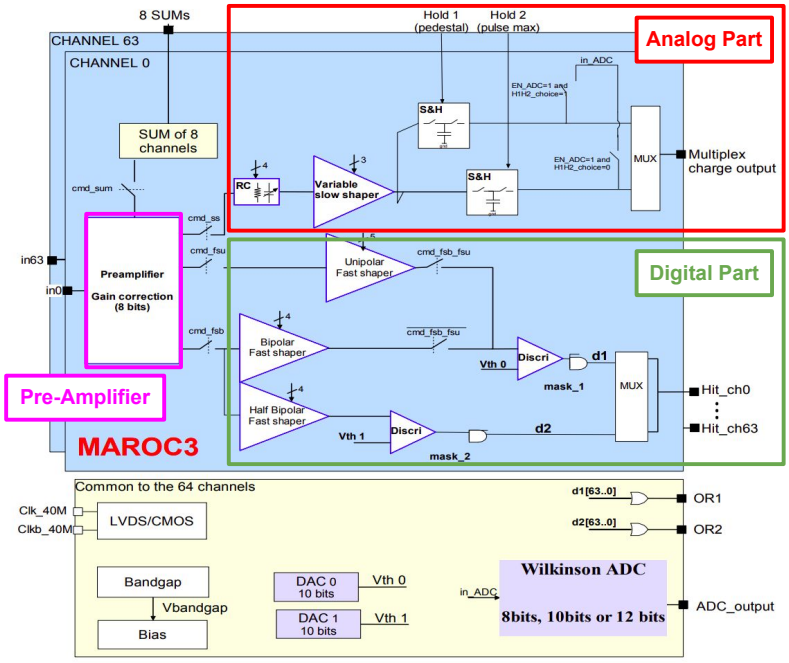

Figure 4. The MAROC3 architecture, see the text for details.

2023 JINST 18 P04013

4 Upgrade of the readout system with SiPMs

During the last CERN long period of shutdown (2019–2021) the detector was inspected and damages to the fiber-PMT connection system were observed, in most of the cases retracted or broken fibers. Since no fiber replacement was possible, it was decided to replace the PMTs with SiPMs, thus allowing us to re-use fibers once the ruined parts have been cut away and the shortened fiber polished again.

SiPMs has demonstrated to be a reliable, affordable and widely used light readout system in the high energy physics environment since a long time. Moreover they are compact, they do not require high voltages and can be operated in magnetic fields.

The chosen SiPM model is ASD RGB-SiPM provided by AdvanSiD.[6] It has an active area of $1 \times 1\,\mathrm{mm}^2$ with a total of 625 cells (cell pitch 40 µm). The device is enclosed in a $2.02 \times 2.48 \times 1.30\,\mathrm{mm}^3$ SMD plastic package covered by a transparent epoxy layer. This model was chosen both for its efficiency absorption spectrum (maximum at 550 nm) that matches the green WLS fibers emission one, and for its radiation hardness [23].

The readout scheme changed from the case where PMTs were used with many fibers readout by a single device, to that with SiPMs where each fiber is connected to its own device, thus requiring both new mechanical interfaces and electronics.

In table 1 a side-by-side comparison of some specification of the old PMT and the chosen SiPM is shown.

Table 1. Comparison of the light readout device used before and after the upgrade of the scintillating bar detector. In the old readout scheme with the PMTs many WLS fibers were readout with one single device whereas after the upgrade one fiber was coupled to a single SiPM with all the mechanical advantages described in the text.

	PMT (H7546B) tube assembly	SIPM (ASD-RGB1S-P)
Manufacturer	Hamamatsu	AdvanSiD
Readout channels	64	1
Dimensions	$30 \times 30 \times 60\,\mathrm{mm}^3$ assembly	$2 \times 2 \times 1.25\,\mathrm{mm}^3$
Effective area	8×8 multianode: $2 \times 2\,\mathrm{mm}^2$/anode	$1 \times 1\,\mathrm{mm}^2$
Operating voltage	−1000 V	30 V
Gain	$10^5 \sim 10^6$	10^6
Dark count rate density	$\sim$100 cps/mm^2	$\sim$100 kcps/mm^2
PDE	~40%	32.5%

5 New electronic board and MAROC3 tests

A new readout board has been designed. It is shown in figure 5: 12 SiPMs have to be surfaced mounted on the dedicated pads and 5 boards, necessary to readout the 60 SiPMs of each panel, are installed very close to the scintillating bars on the internal frame. Each channel is equipped

[6] https://advansid.com/home.

2023 JINST 18 P04013

with one dual AD8002 current feedback amplifier and the necessary passive circuitry; moreover its footprint matches the bar cross section. The signals are then brought to the FEB using ~50 cm Hirose U.FL series thin coaxial cables[7] and plugged into an adapter board designed to mimic the 8×8 array geometry of the old multi-anode PMT socket.

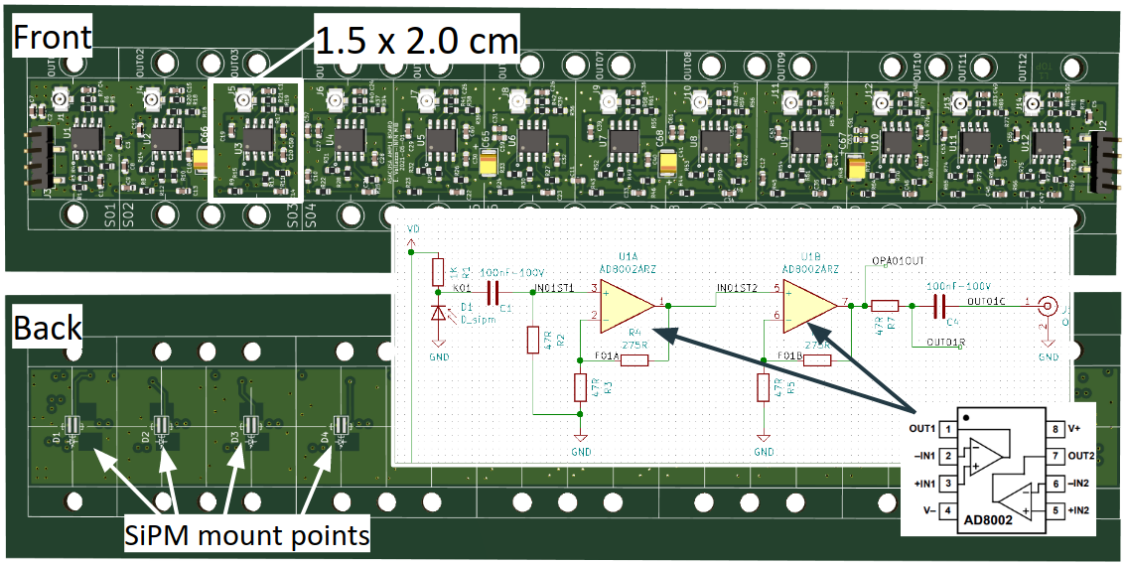

Figure 5. Drawing of the new 12 SiPM readout front-end board. The design of a single channel is overlapped together with the AD8002 amplifier scheme: each SiPM anode is connected to ground while the cathode is positively biased and connected to a capacitor. The SiPM current pulse generates a voltage signal (through the capacitor) which is amplified.

All the WLS fibers have been shortened down to a ~6–8 cm length, polished and then glued onto a 3D printed connector (see the next section 6) whose counterpart is directly fixed to the new SiPM front-end board.

Different tests were performed to compare the behaviour of the ASIC with the one described in the datasheet. Using a pulse generator, a step function signal of 1 V was injected in the calibration input of the MAROC3 after a 2.2 pF capacitor to test all its channels; the multiplexed digitized output was readout by a VME control board synchronized with the pulse generator. Loading the MAROC3 mask with the configuration of the analog circuit, different scans of the hold value were performed, as well as of the shaper capacitors values and of different preamplifier gains.

The scan of the hold parameter values allows to reconstruct the analog signal shape varying the time at which the signal is sampled with respect to the trigger. The result is shown in figure 6: 40 steps of 3.3 ns hold values were chosen in the (3.3, 1290) ns range and 200 events per step were acquired. The gain was set to 128 and the slow shaper capacitor to 900 fF.

The shaper scan was performed varying the value of the slow shaper capacitor in the (300, 2100) fF range for a fixed gain value of 128. For every capacitance chosen, a hold scan (like the one explained above) was done to record the shapes of the signal. An example of the shaper scan for the 11th channel is shown in figure 7, where the change in the shape and in the amplitude is visible.

[7] https://www.hirose.com/product/series/U.FL.

2023 JINST 18 P04013

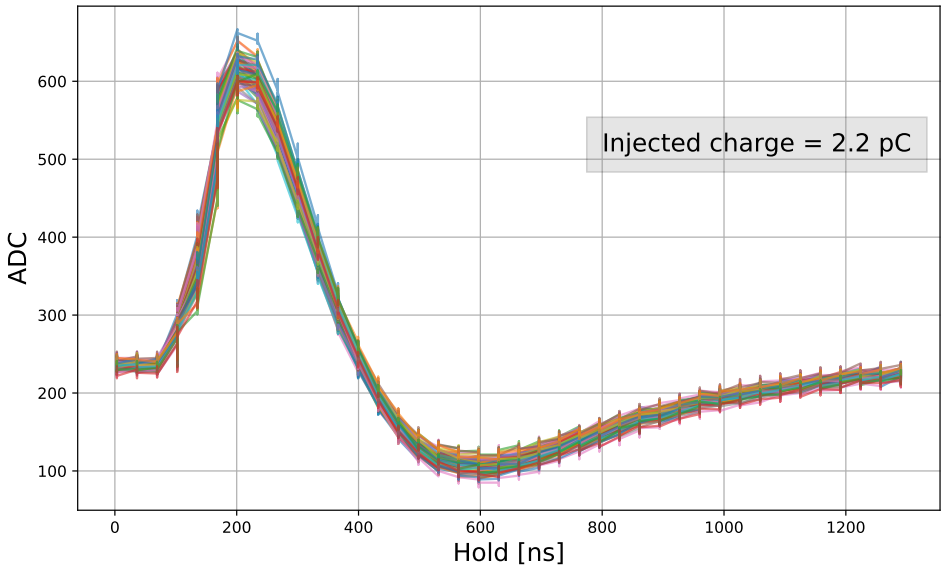

Figure 6. The hold scan of all the MAROC3 channels.

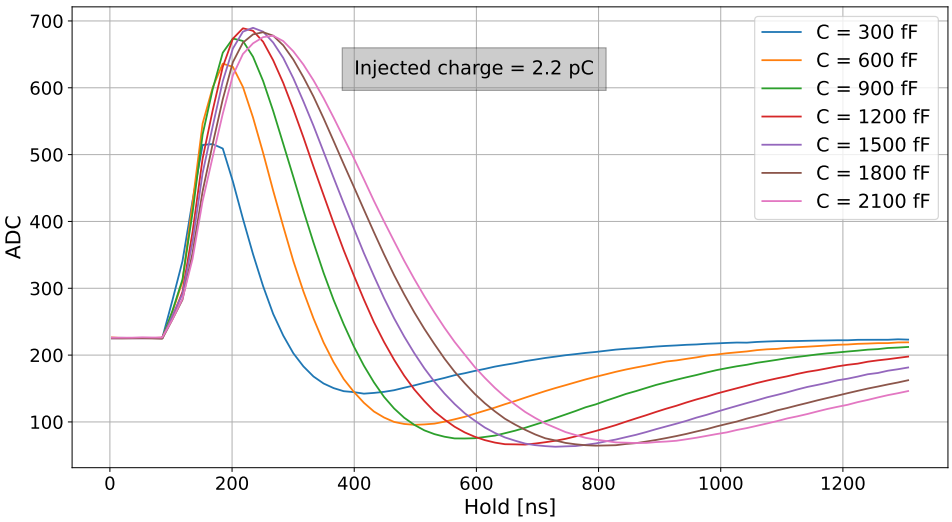

Figure 7. The shaper scan of the MAROC3 11th channel for different slow shaper capacitors.

In figure 8, the average amplitude of the signal of all the MAROC3 channels and their peaking times are shown as a function of the different slow shaper capacitance values chosen for the scan.

Two scans of the preamplifier gain values were performed: one to verify the linearity behaviour of the signal amplitude as a function of the gain and the other to study the response of the preamplifier for different gains and input signal magnitudes. For both tests, the amplitude was measured performing the hold scan described above for every case and the slow shaper capacitor was set to 900 fF. The linearity is verified for all the preamplifier gains, as shown in the inset plot of figure 9; in the main plot a saturation effect is visible for all the three gain values for input signals above ~3 V, but a good linearity is present before that value as underlined by the linear fit shown in black in the same figure 9.

2023 JINST 18 P04013

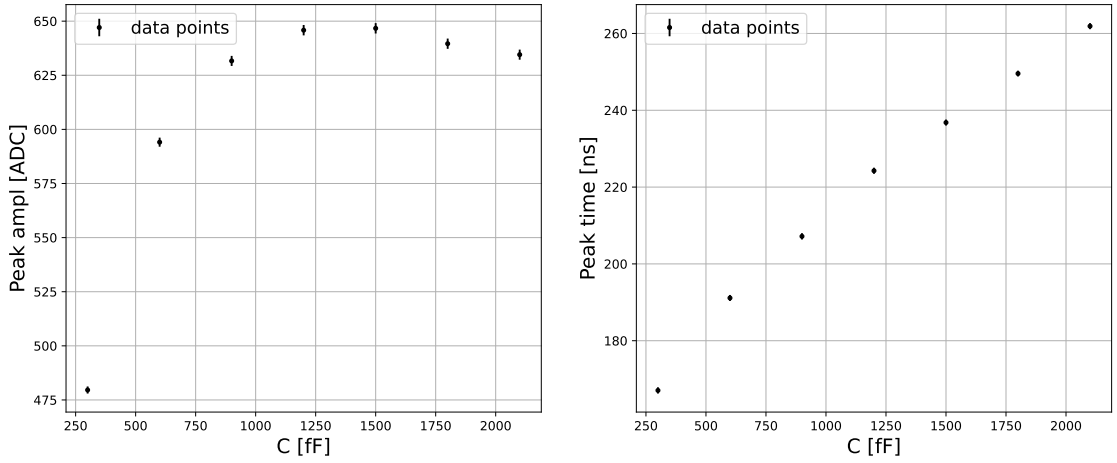

Figure 8. The shaper scan of a channel of the MAROC3 for different slow shaper capacitors.

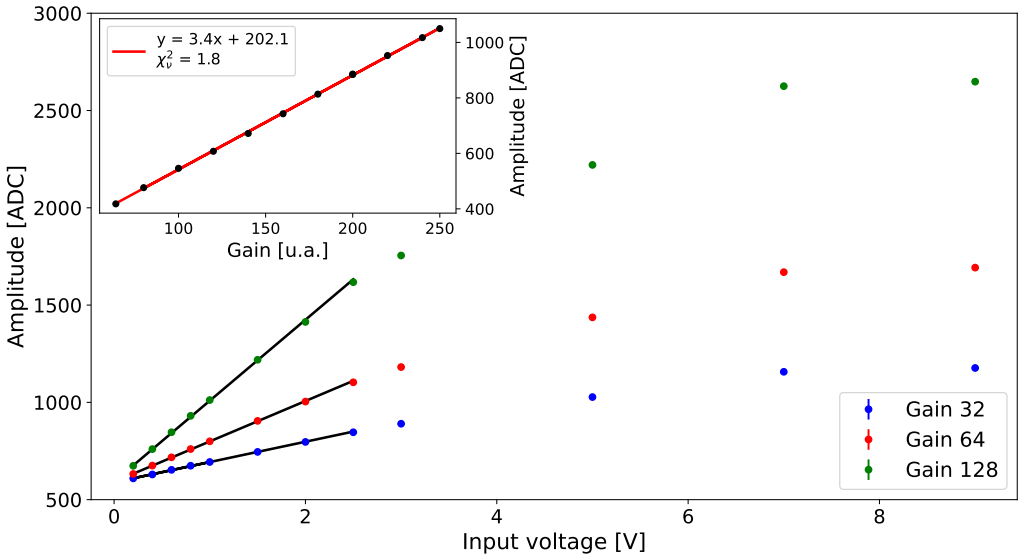

Figure 9. Linearity test for the MAROC3 preamplifier. Main plot: scan of different input signals for 3 gain values; the black line represents a linear fit of the data up to 3 V, beyond that value a saturation is present. Inset: scan of different preamplifier gain values and the linear fit in red.

The final configuration of the MAROC3 parameters for the readout of the scintillating bar detector was chosen as follows:

- since the SiPMs signals are already pre-amplified on the SiPM frontend boards and to prevent saturation of the ADC on the MAROC3 board, we choose a low preamplifier gain;
- the buffer and the slow shaper were set in the slowest configuration, i.e. with the highest capacitance, to have the longest shaping time. This configuration allowed us to hold the signal correctly, since the trigger logic takes time to generate the busy signal for the sample-and-hold circuit.

2023 JINST 18 P04013

6 Mechanical upgrades

In order to align the WLS fibers to the SiPMs' active surface, an optical coupler was designed and moulded in resin using a Project 2500 Pro machine by 3D System[8] that works with material jetting technology thus offering the required resolution. The ink-jet printing process uses piezo print-head technology to deposit photo-curable plastic resin droplets layer by layer and wax is used as support material. At the end the parts are immersed in mineral oil and undergo ultrasonic cleaning.

The coupler, shown in figure 10 is composed by two parts: the first has a cylindrical shape with a circular hole to allow the gluing of the WLS fiber end cap, whereas the second one is a counterpart where the cylinder with the fiber has to be housed.

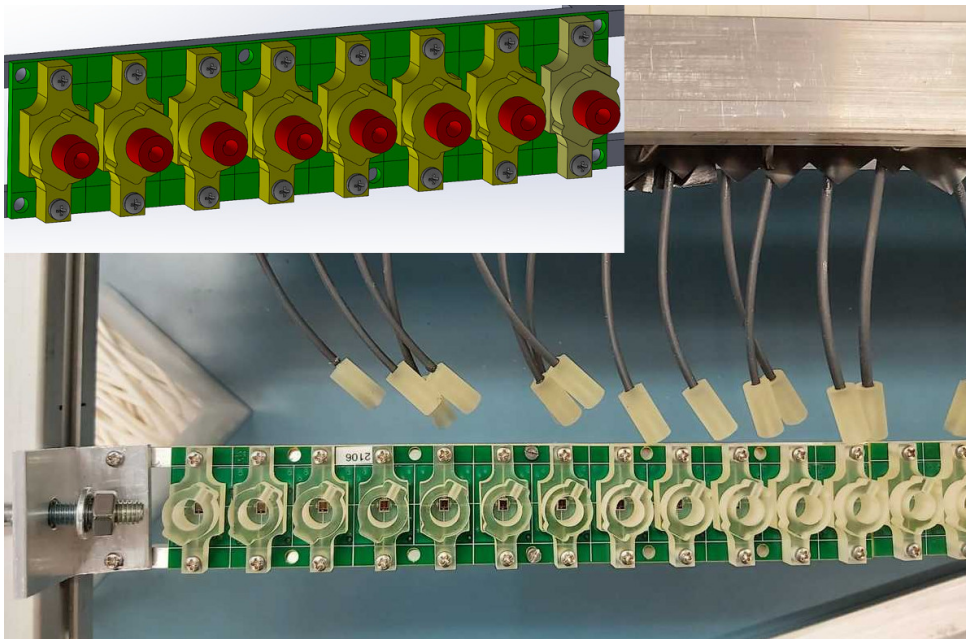

Figure 10. 3D scheme of the coupling between the two resin couplers (the ocher and the red parts) and the electronic board (green part) on which the SiPMs are fixed.

The internal mechanical supports were refurbished in order to keep the new SiPM front-end boards at a fixed distance and position with respect to the scintillating bars so that the fiber curvature is minimized and no stress is applied when the detector is moved and vibrations propagate to all its parts. In figure 11 a particular of the new framing system is shown.

7 Test with cosmic rays

In order to evaluate the detector performances, the panels have been stacked in the laboratory and tested with cosmic rays. A scheme of the used setup is shown in figure 12: the incoming muons hit plastic scintillators which provide the trigger to the DAQ; the muon track is determined using two ~50 µm resolution microstrip detectors with an active surface of $\sim 18 \times 18\,\mathrm{cm}^2$ [24]. The expected muon hit position on a given panel is computed by extrapolating the track intersection with the

[8] https://www.3dsystems.com/.

2023 JINST 18 P04013

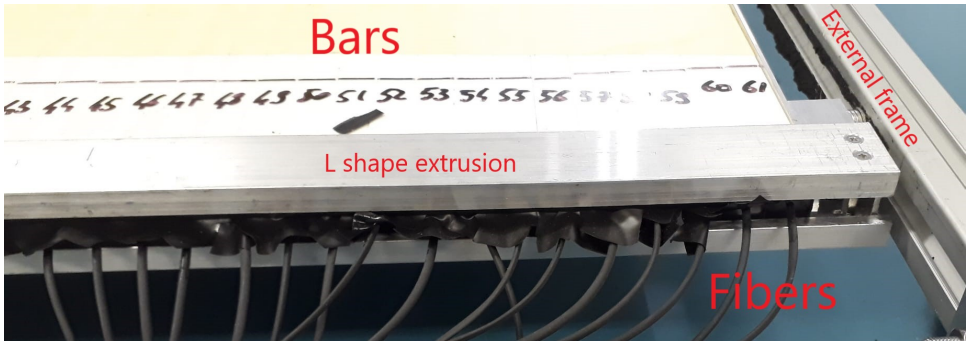

Figure 11. New mechanical support. The scintillating bars are held by 2 L-shaped aluminium extrusions tied together and hinged to the external aluminium frame, to obtain a self-supporting system.

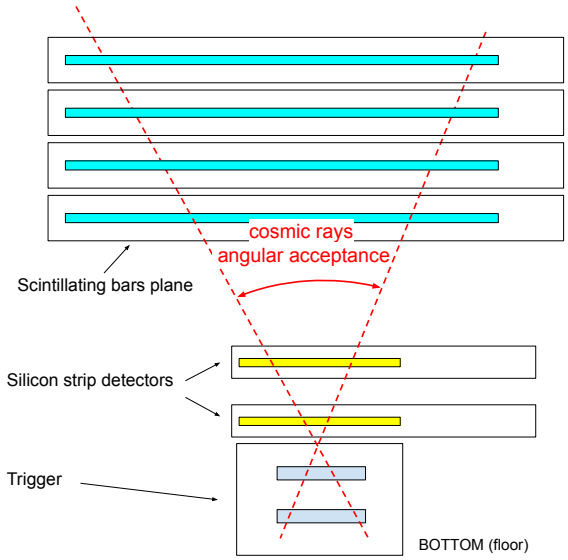

Figure 12. Scheme of the setup used in the laboratory to test the scintillating panels.

panel plane. The obtained spatial resolution of the reconstructed hit point is ~6 mm for all the panels, which is slightly worse than the expected value for particles always crossing one single bar (1.5 cm bar width / $\sqrt{12}$ = 4.3 mm), nevertheless this result represents an improvement with respect to the 10 mm measured with the old PMT system [9]. An efficiency map for all panels can be computed counting each time a given track is detected or not on the expected position. The resulting distributions are shown in figure 13. In order to define a panel efficiency, the median value of all channel efficiency is shown on the plots. The efficiency is clearly not uniform for all the tested panels, regions of poor light yield probably due to a poor fiber-SiPM coupling are clearly visible. Nevertheless the test allows an intervention to fix poor connections before the commissioning and the installation of the detector in the experimental area. The obtained result of 85–90% does not represent an improvement with respect to the value obtained years ago, which was around 93% [9]. But it has to be noticed that the already mentioned detector damages (moved bars, broken or bent fibers) would have made almost impossible those results to be reproduced, leading to the decision

2023 JINST 18 P04013

of the replacing the light readout system. Moreover, the experiment does not require a very high efficiency whereas a good uniformity along the panels is more valuable (achievable after the already mentioned intervention). Indeed, an improvement of the overall efficiency was not expected from the upgrade, which was primarily intended to cope with the irreversible mechanical damages to the detector while preserving as much as the existing front-end electronics.

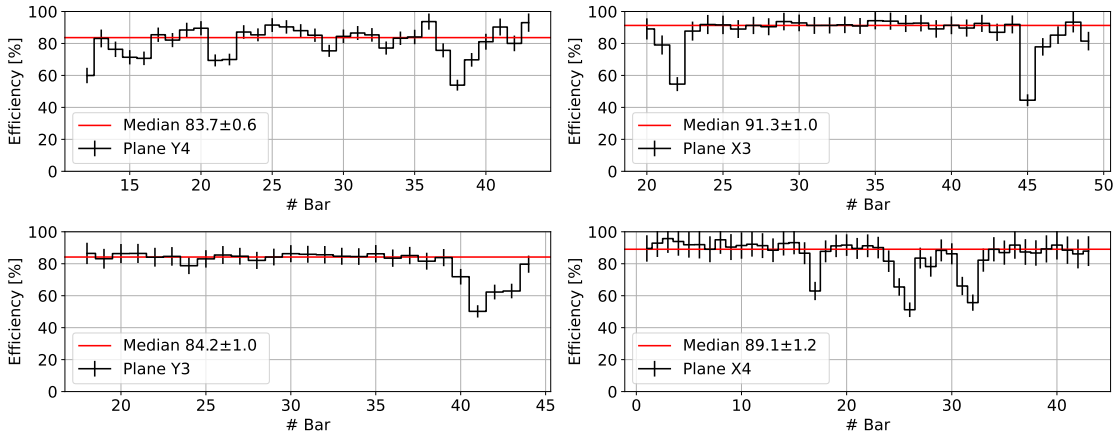

Figure 13. Efficiency as a function of the hit channel for the 4 panels tested with cosmic rays. The channel number is represented on the abscissa and different among the panels because of their different acceptance range (see the scheme in figure 12).

8 Conclusions

The scintillating bar detector for the ASACUSA experiment has been recently upgraded. A SiPM based light readout system have been designed and tested toghether with new front-end electronics board and a refurbished internal mechanical structure to replace the multi-anode photomultipliers. All the necessary tests on the new electronics have been performed, as well as a data taking period with cosmic rays. The commissioning phase has finished and the detectors will be soon installed in the experimental area for the data taking.

References

[1] Y. Enomoto et al., *Synthesis of Cold Antihydrogen in a Cusp Trap*, *Phys. Rev. Lett.* **105** (2010) 243401.

[2] ASACUSA collaboration, *A source of antihydrogen for in-flight hyperfine spectroscopy*, *Nature Commun.* **5** (2014) 3089.

[3] C. Malbrunot et al., *The ASACUSA antihydrogen and hydrogen program : results and prospects*, *Phil. Trans. Roy. Soc. Lond. A* **376** (2018) 20170273 [arXiv:1710.03288].

[4] B. Kolbinger et al., *Measurement of the principal quantum number distribution in a beam of antihydrogen atoms*, *Eur. Phys. J. D* **75** (2021) 91 [arXiv:2008.04246].

[5] ASACUSA collaboration, *Two-photon laser spectroscopy of antiprotonic helium and the antiproton-to-electron mass ratio*, *Nature* **475** (2011) 484 [arXiv:1304.4330].

2023 JINST 18 P04013

[6] ASACUSA collaboration, *Buffer-gas cooling of antiprotonic helium to 1.5 to 1.7 K, and antiproton-to-electron mass ratio*, *Science* **354** (2016) 610.

[7] A. Sótér, H. Aghai-Khozani, D. Barna, A. Dax, L. Venturelli and M. Hori, *High-resolution laser resonances of antiprotonic helium in superfluid ^{4}He*, *Nature* **603** (2022) 411.

[8] G. Bendiscioli and D. Kharzeev, *Anti-nucleon nucleon and anti-nucleon nucleus interaction: A Review of experimental data*, *Riv. Nuovo Cim.* **17N6** (1994) 1.

[9] M. Corradini et al., *Scintillating bar detector for antiproton annihilations measurements*, *Hyperfine Interact.* **233** (2015) 53.

[10] Y. Enomoto et al., *Synthesis of Cold Antihydrogen in a Cusp Trap*, *Phys. Rev. Lett.* **105** (2010) 243401.

[11] Y. Nagata et al., *Direct detection of antihydrogen atoms using a BGO crystal*, *Nucl. Instrum. Meth. A* **840** (2016) 153.

[12] C. Sauerzopf et al., *Towards measuring the ground state hyperfine splitting of antihydrogen – a progress report*, *Hyperfine Interact.* **237** (2016) 103 [arXiv:1606.01791].

[13] Asacusa collaboration, *Recent Developments from ASACUSA on Antihydrogen Detection*, *EPJ Web Conf.* **181** (2018) 01003.

[14] ASACUSA collaboration, *Hyperfine spectroscopy of hydrogen and antihydrogen in ASACUSA*, *Hyperfine Interact.* **240** (2019) 5 [arXiv:1809.00875].

[15] H. Aghai-Khozani et al., *Measurement of the antiproton-nucleus annihilation cross-section at low energy*, *Nucl. Phys. A* **970** (2018) 366.

[16] K. Todoroki et al., *Instrumentation for measurement of in-flight annihilations of 130 keV antiprotons on thin target foils*, *Nucl. Instrum. Meth. A* **835** (2016) 110.

[17] H. Aghai-Khozani et al., *First experimental detection of antiproton in-flight annihilation on nuclei at similar 130-keV*, *Eur. Phys. J. Plus* **127** (2012) 125.

[18] H. Aghai-Khozani et al., *First measurement of the antiproton-nucleus annihilation cross section at 125 keV*, *Hyperfine Interact.* **234** (2015) 85.

[19] H. Aghai-Khozani et al., *Limits on antiproton-nuclei annihilation cross sections at ~125 keV*, *Nucl. Phys. A* **1009** (2021) 122170.

[20] A. Pla-Dalmau, A.D. Bross and K.L. Mellott, *Low-cost extruded plastic scintillator*, *Nucl. Instrum. Meth. A* **466** (2001) 482.

[21] P. Jenni, M. Nordberg, M. Nessi and K. Jon-And, *ATLAS Forward Detectors for Measurement of Elastic Scattering and Luminosity*, CERN-LHCC-2008-004 (2008).

[22] S. Blin, P. Barrillon and C. de La Taille, *MAROC, a generic photomultiplier readout chip*, 2010 *JINST* **5** C12007.

[23] F. Acerbi et al., *Irradiation and performance of RGB-HD Silicon Photomultipliers for calorimetric applications*, 2019 *JINST* **14** P02029 [arXiv:1901.08430].

[24] M. Prest et al., *The AGILE silicon tracker: An innovative gamma-ray instrument for space*, *Nucl. Instrum. Meth. A* **501** (2003) 280.

2023 JINST 18 P04013